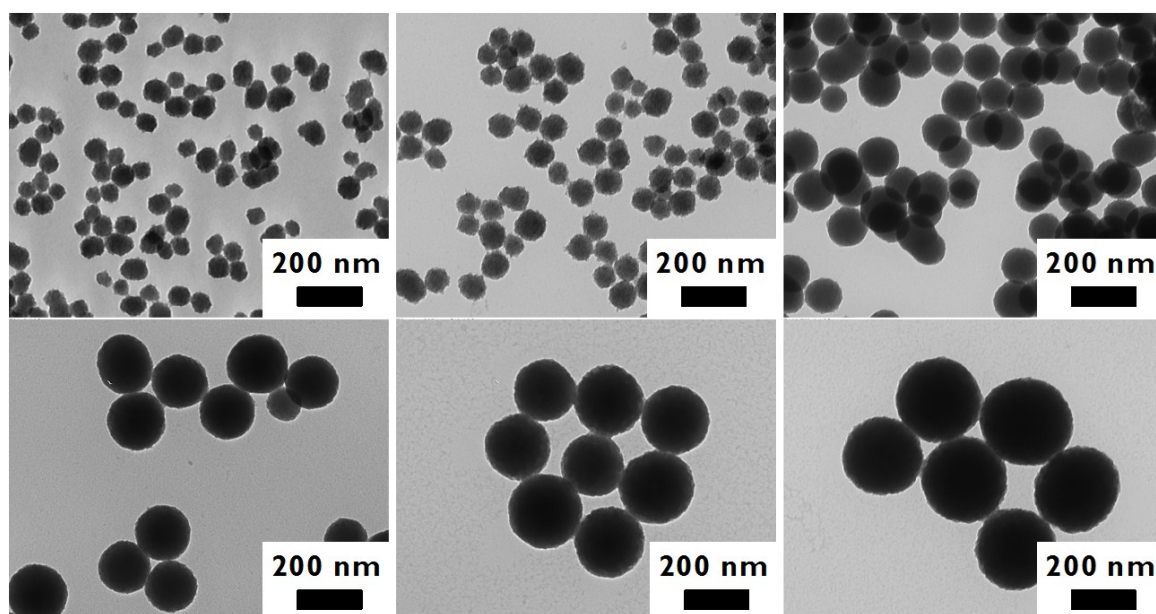


## Supporting Information

### Simple Size Control of TiO<sub>2</sub> Nanoparticles and Their Electrochemical Performance: Emphasizing the Contribution of Surface Area to Lithium Storage at High-Rates

*Joohyun Lim, Ji Hyun Um, Kyung Jae Lee, Seung-Ho Yu, Young-Jae Kim, Yung-Eun Sung\*, and Jin-Kyu Lee\**



**Figure S1.** TEM images of size-tunable TNPs ranging in particle size from approximately 60 nm to 300 nm.

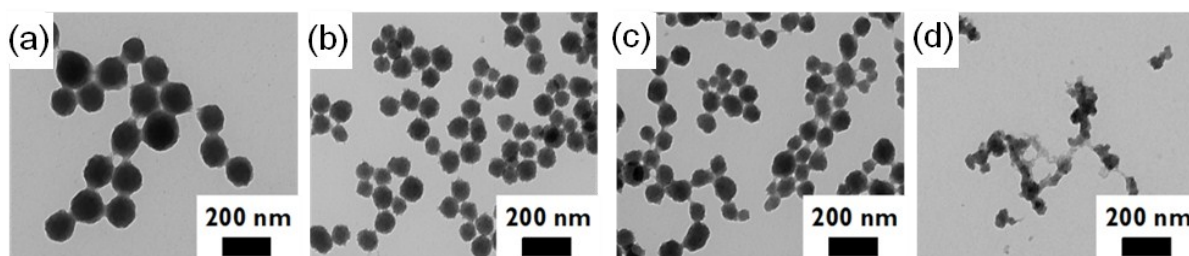


**Figure S2.** TEM images of TNPs using varying amounts of water: a) 0.025 mL, b) 0.05 mL, c) 0.1 mL and d) 0.2 mL. Other reaction conditions were the same, as follows: 2 mL of diluted  $\text{Ti}(\text{O}i\text{Bu})_4$  solution, 0.05 mL of ammonia solution in 1:1 (v/v) mixture of ethanol:acetonitrile solution (10 mL).

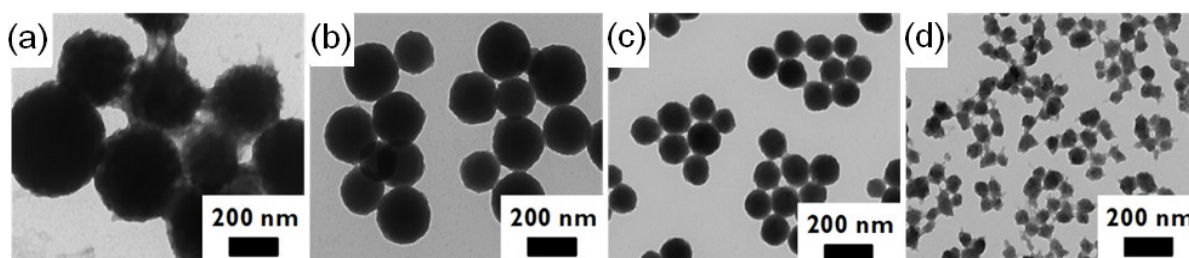


**Figure S3.** TEM images of TNPs using varying amounts of ammonia solution: a) 0.025 mL, b) 0.05 mL, c) 0.1 mL and d) 0.2 mL. Other reaction conditions were the same as follows: 2 mL of diluted  $\text{Ti}(\text{O}i\text{Bu})_4$  solution, in 1:1 (v/v) mixture of ethanol:acetonitrile solution (10 mL).

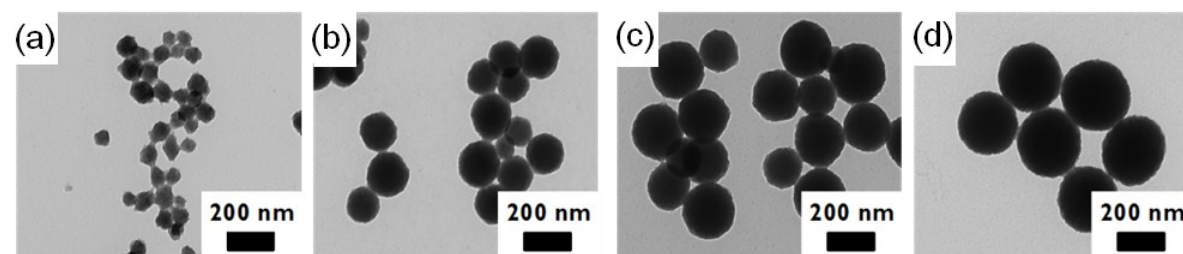


**Figure S4.** TEM images of TNPs using varying amounts of diluted  $\text{Ti}(\text{O}i\text{Bu})_4$  solution: a) 0.025 mL, b) 0.05 mL, c) 0.1 mL and d) 0.2 mL. Other reaction conditions were the same as follows: 2 mL of diluted  $\text{Ti}(\text{O}i\text{Bu})_4$  solution, 0.05 mL of ammonia solution in 1:1 (v/v) mixture of ethanol:acetonitrile solution (10 mL).

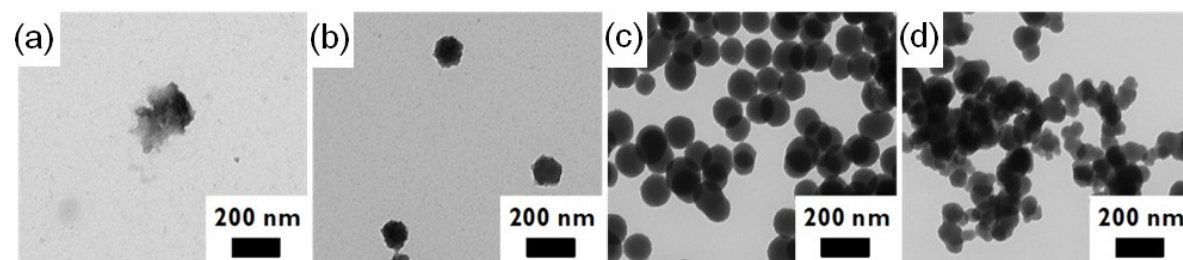


**Figure S5.** TEM images of TNPs using varying ratios of ethanol and acetonitrile (v/v): (a) 9:1, (b) 3:1, (c) 1:3, and (d) 1:9. Other reaction conditions were the same as follows: 2 mL of diluted  $\text{Ti}(\text{O}i\text{Bu})_4$  solution, 0.05 mL of ammonia solution.

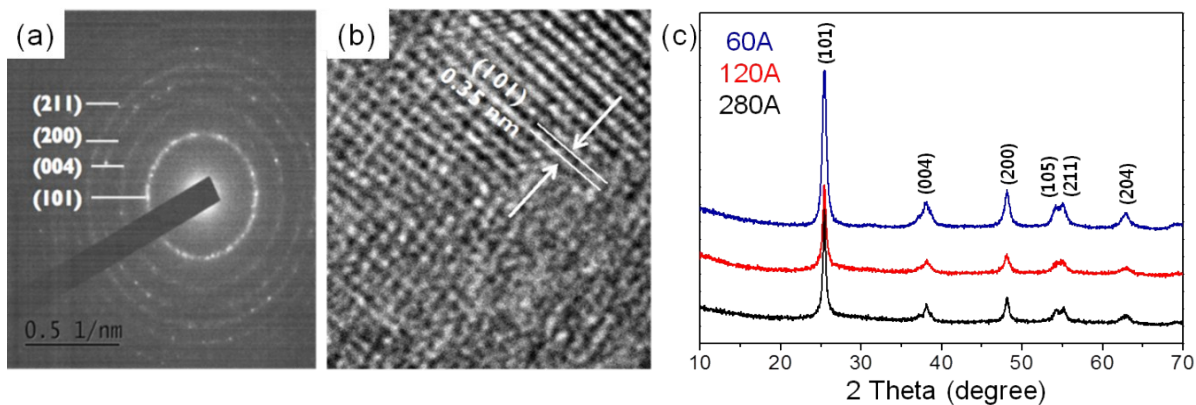


**Figure S6.** a) Electron diffraction patterns from annealed 60 nm TNPs, which were assigned to the pure anatase phase and b) lattice fringe of (101) XRD patterns of TNPs, which could also be identified with the pure anatase phase. c) XRD patterns of TNPs with sizes of 60 nm, 120 nm, and 280 nm.

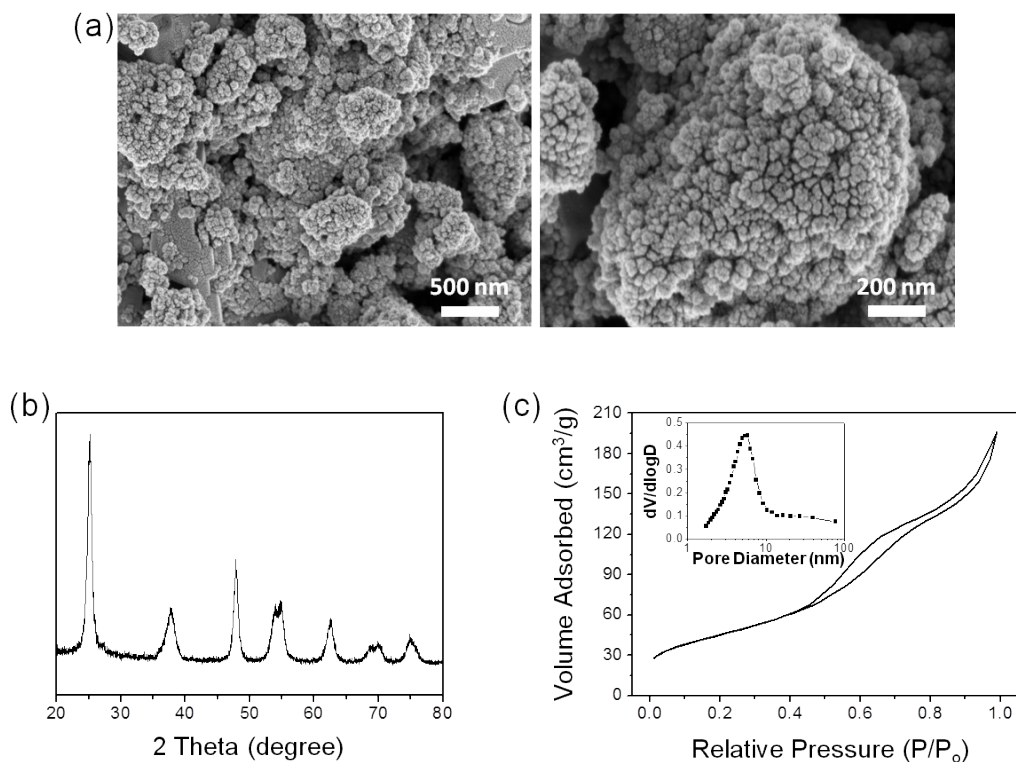


**Figure S7.** Characterizations of commercial  $\text{TiO}_2$  nanopowder of a) SEM images, b) XRD pattern, and c) nitrogen adsorption/desorption isotherm with the inset of BJH pore size distributions.

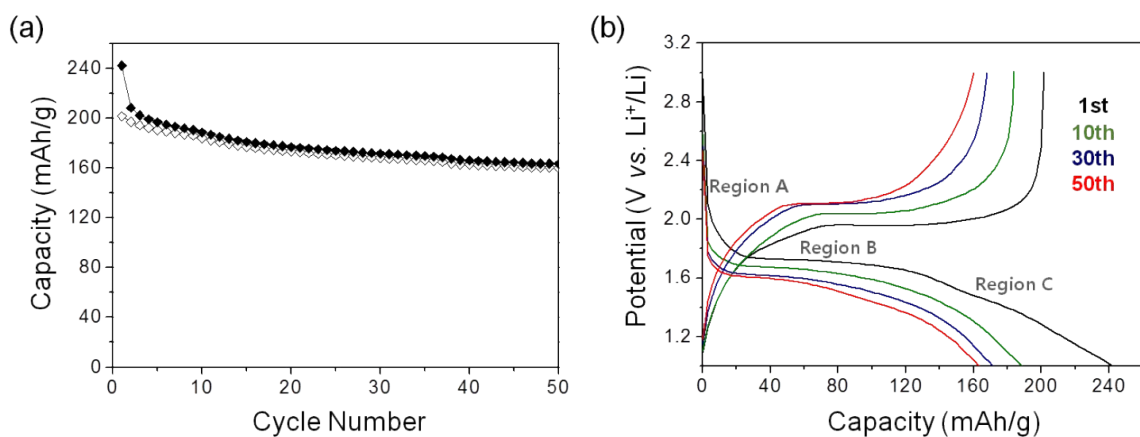


**Figure S8.** a) Cycle performance of the commercial  $\text{TiO}_2$  nanopowder at 1 C for 50 cycles and b) voltage profiles at the selected cycles.

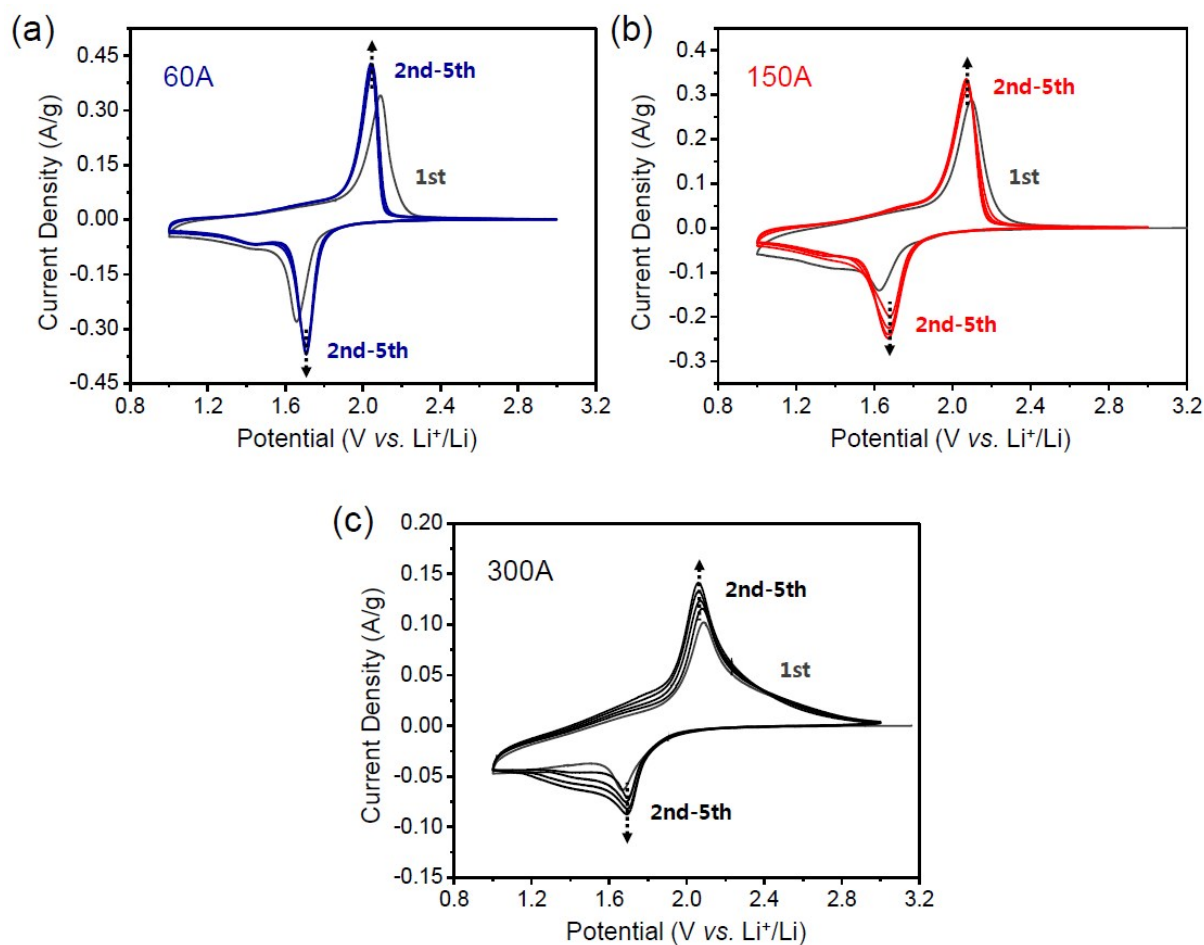


**Figure S9.** Cyclic voltammograms of a) 60A, b) 120A, and c) 280A at a scan rate of 0.1 mV/s.

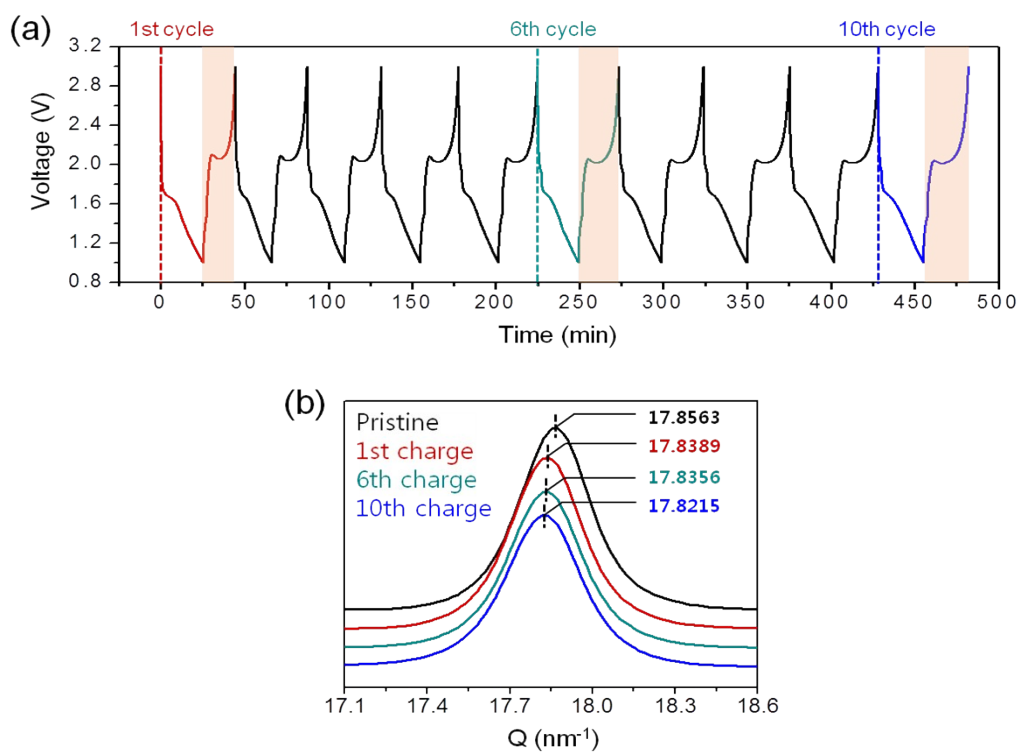


**Figure S10.** a) Voltage profiles of the 280 during 10 cycles and b) in-situ XRD patterns of the 280A at the selected cycle.

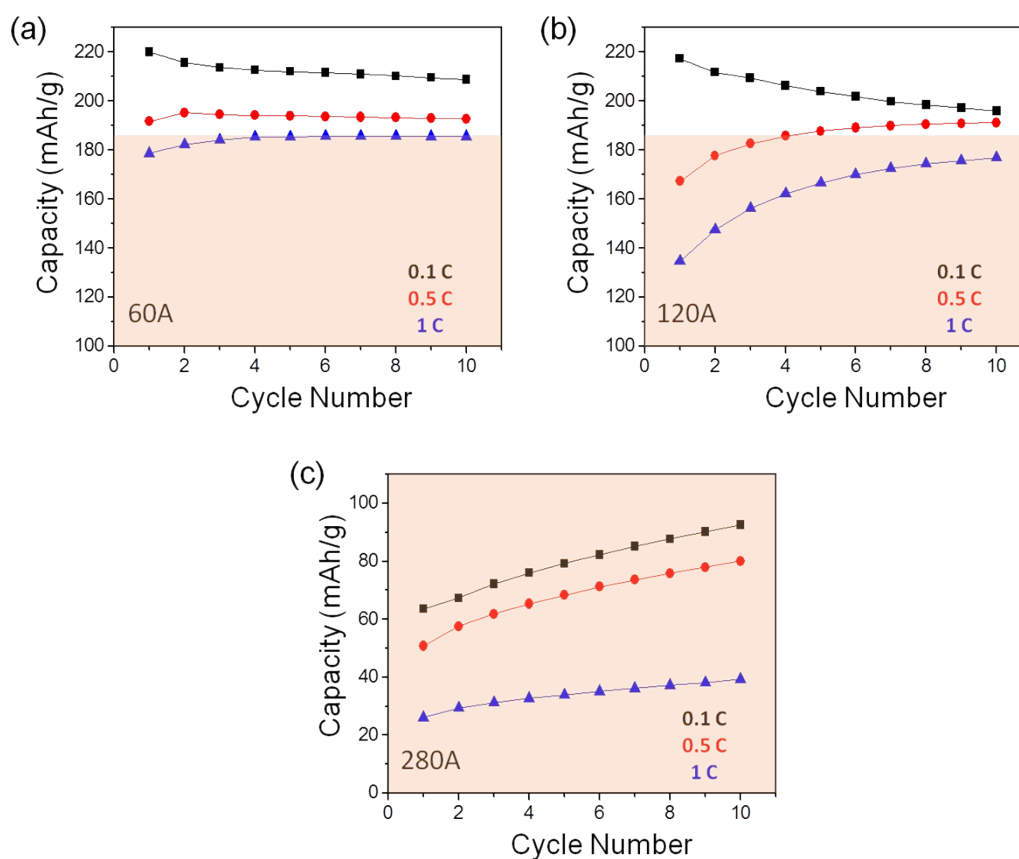


**Figure S11.** The charge capacity of the size-controlled TNPs at different C-rates during 10 cycles.

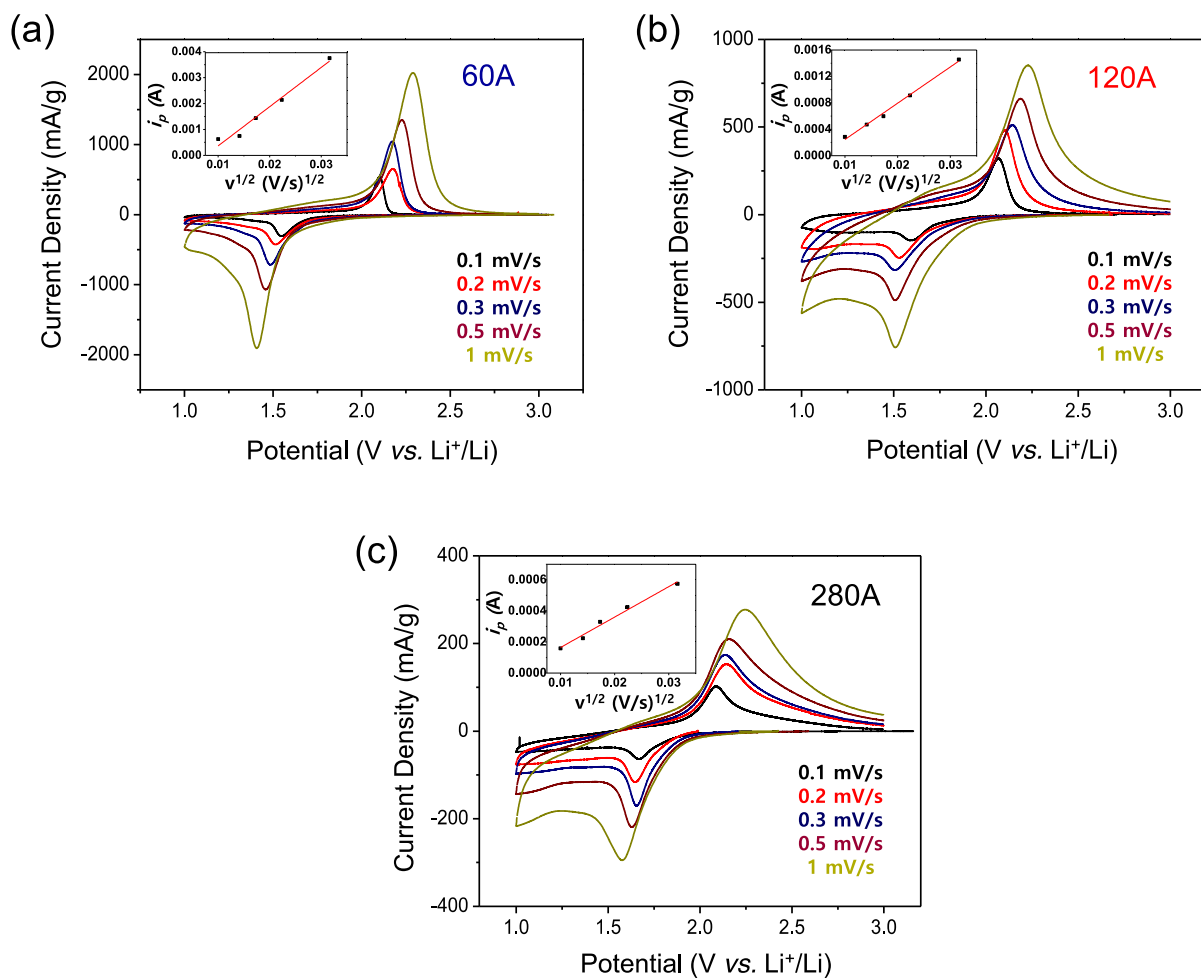


**Figure S12.** Cyclic voltammograms of a) 60A, b) 120A, and c) 280A with varying scanning rates of 0.1, 0.2, 0.3, 0.5, and 1 mV/s. The correlation line of  $i_p$  vs.  $v^{1/2}$  is displayed in the inset.

**Table S1** Structural properties of the size-controlled TNPs.

TNPs	60A	120A	280A
SSA (BET) <sup>a)</sup> [m <sup>2</sup> /g]	73	46	41
The major pore size within several nanometers (BJH) <sup>b)</sup> [nm]	4	4	4
The major pore size with tens of nanometers (BJH) [nm]	26	52	n.m. <sup>f)</sup>
SSA (Hg) <sup>c)</sup> [m <sup>2</sup> /g]	32	17	6
The major pore size within several nanometers (Hg) [nm]	n.m. <sup>f)</sup>	n.m. <sup>f)</sup>	n.m. <sup>f)</sup>
The major pore size with tens of nanometers (Hg) [nm]	14	21	40
Interparticle pore size <sup>d)</sup> [nm]	25	50	116
Crystallite size (XRD) <sup>e)</sup> [nm]	12	12	13
Particle size (TEM) [nm]	60	120	280

<sup>a)</sup>SSA = specific surface area; BET = Brunauer–Emmett–Teller,

<sup>b)</sup>BJH = Barrett–Joyner–Halenda,

<sup>c)</sup>SSA = specific surface area; Mercury Intrusion Porosimetry,

<sup>d)</sup>calculated pore size from the hexagonal close packed sphere,

<sup>e)</sup>determined by the Scherrer equation,

<sup>f)</sup>n.m. = not measurable.

**Table S2** Comparison of the capacity at 10 C of TiO<sub>2</sub>-based materials reported in literatures and this work.

Material	Current density (mA/g)	Capacity (mAh/g)	Reference
60 nm TiO <sub>2</sub> nanosphere	1680	120	[Our work]
TiO <sub>2</sub> nanocage	1700	85	39
TiO <sub>2</sub> hollow sphere	1730	105.6	40
Mesoporous TiO <sub>2</sub>	1680	~137	41
TiO <sub>2</sub> from metal-organic framework	1680	~110	42
TiO <sub>2</sub> on reduced graphene oxide	1005	143	43
	2010	118	
N, S doped TiO <sub>2</sub>	1680	63.5	44
Carbon nanotube/mesoporous TiO <sub>2</sub> coaxial nanocables	1680	112	45
Carbon-coated mesoporous TiO <sub>2</sub> nanocrystals on graphene	1000	~80	46
	2000	~75	
Hollow TiO <sub>2</sub> /graphitic carbon	1000	151	47
	2000	131	

**Table S3** Li ion diffusion coefficients from the slow-scan cyclic voltammetry method.

TNPs	$D_{Li^+}$ [cm <sup>2</sup> /s]
60A	$8.12 \times 10^{-20}$
120A	$1.60 \times 10^{-20}$
280A	$1.32 \times 10^{-21}$